Continuously Variable True Time-Delay Optical Feeder for Phased-Array Antenna Employing Chirped Fiber Gratings

J. L. Corral, J. Martí, *Member, IEEE*, S. Regidor, J. M. Fuster, R. Laming, and M. J. Cole

***Abstract*— In this paper, we present and demonstrate a novel approach of a true time-delay (TTD) optical feeder for phased-array antennas (PAA's). A continuously variable TTD is achieved by employing tunable lasers and a wide-bandwidth chirped fiber Bragg grating (FBG) as the dispersive element. The results show that a very high resolution performance (equivalent to a 6-b microwave phase shifter) is obtained for an L-band PAA employing narrow-tuning bandwidth lasers with a wavelength stability of 0.005 nm and a 4-nm bandwidth chirped grating with a dispersion of 835 ps/nm.**

***Index Terms*— Chirped fiber gratings, phased array, optical beamforming, true time delay.**

I. Introduction

THE USE OF optical fiber in phased-array antennas (PAA's) has been deeply considered for beamforming, signal distribution, and antenna-element synchronization [1]. Its advantages are quite well known: small size, low losses, lightweight, wide instantaneous bandwidth, and immunity to electromagnetic interferences. One key concept in a PAA is to find a phase-shift element which could show features such as size compactness, low losses, continuous variability, high flexibility, and true time delay (TTD) (thus allowing broad-bandwidth squint-free operation). Phase-shift selection based on wavelength-switching has been proposed by using dispersive fiber [2]–[4] to generate relative time delay among the optical wavelengths. Fiber Bragg gratings (FBG's) have also been used as wavelength-selective time-delay elements [5]–[7] relying on their wavelength-dependent reflective properties in such a way that by carefully selecting the FBG position, each wavelength is associated with a different round-trip time delay. Instead of using several FBG's at different discrete positions, we propose a TTD optical feeder scheme which employs only one wide-bandwidth chirped FBG. In this approach, since each wavelength is reflected at a different position along the grating length, by tuning the laser wavelength the time delay is selected on an almost continuous way. Recently, a very wide-bandwidth (4-nm) chirped FBG has been fabricated [8], which will allow many array antenna elements as well as moderate wavelength tolerances for the lasers. Even though the use of a chirped FBG has been proposed [5], [6], it has not yet been demonstrated, and its continuous group-delay compactness features have not been exploited. The difference between previously proposed optical feeders for PAA [2]–[6] and the approach presented in this paper is that this approach allows *any* possible antenna-element phase distribution (not just linear phase), making it suitable for advanced PAA features as selective nulling techniques.

The paper is organized as follows. The principle of the TTD scheme is presented in Section II. In Section III, that scheme is demonstrated, as well as the impact of the inaccuracies due to the wavelength laser stability, and the linearity of the chirped FBG on the PAA performance is considered. Remarks and discussion on the grating-based optical feeder are reported in Section IV. Finally, a conclusion is provided in Section V.

II. Principle

The transmitting setup of the proposed TTD optical feeder is shown in Fig. 1. A wavelength-to-array-element correspondence is used. The output lights of N narrow-tuning bandwidth tunable lasers (λ_1 to λ_N) are combined and all the optical wavelengths are modulated by the same microwave signal employing a external electro-optic modulator (EOM). The modulated lightwaves pass through an optical circulator to a long (several centimeters) wide-bandwidth chirped FBG. The resonance position inside the FBG, i.e., the reflection point, depends on the wavelength according to the selected chirping law. If a linear chirp is chosen, the relation between the reflection position and the wavelength is linear, and so is the round-trip delay. Fig. 2 schematically shows the group delay of a linear chirped FBG connected as shown in Fig. 1. In Fig. 2, it may be observed that the shorter the wavelength is, the closer the resonance takes place, and the lower the time delay is. The N delayed modulated optical carriers, λ_1 to λ_N are separated by a means of a wavelength-division-multiplexed (WDM) demultiplexer and then passed to each antenna element after photodetection (PD). Depending on the specific values of optical bandwidth and optical carrier's separation, the WDM demultiplexer may be implemented as an $1 \times N$ optical coupler and N narrow-band unchirped grating filters.

Manuscript received December 10, 1996; revised April 23, 1997. This work was supported in part by Pirelli Cavi SpA and in part by the Spanish Research Commission (CICYT) through the projects TIC95-0859-C02–01 and TIC 96–0611.

J. L. Corral, J. Martí, S. Regidor, and J. M. Fuster are with ETSI Telecomunicacion, Universitat Politecnica de Valencia, 46071 Valencia, Spain.

R. Laming and M. J. Cole are with Optoelectronics Research Centre, Southampton University, Southampton, SO17 1BJ, U.K.

Publisher Item Identifier S 0018-9480(97)05995-4.

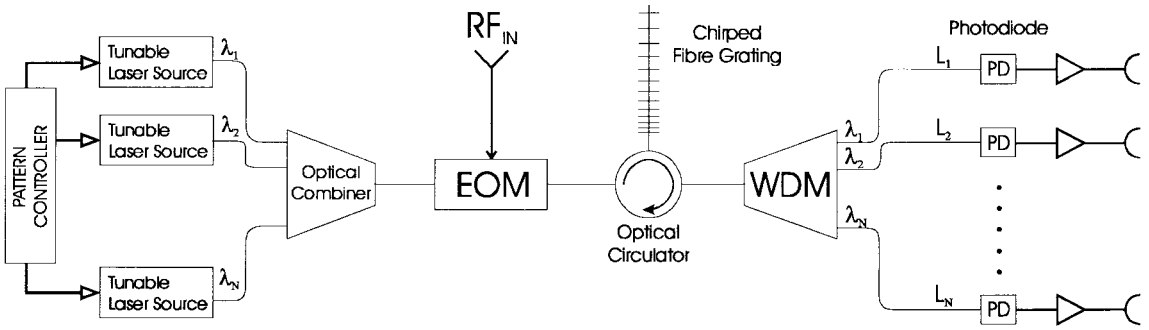

Fig. 1. TTD beamformer transmitting-mode block diagram.

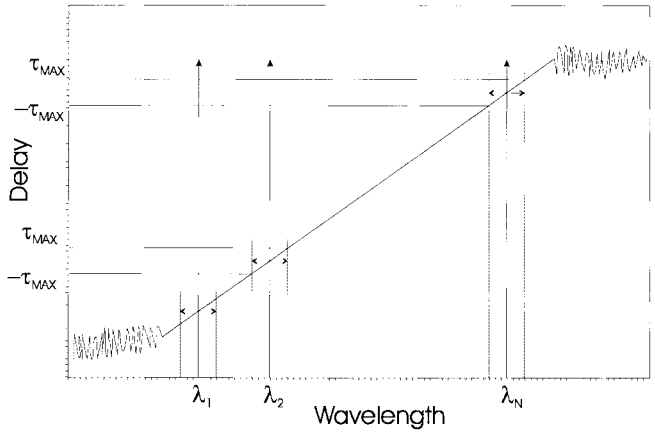

Fig. 2. Fiber-grating group-delay response and nominal wavelength placement, showing available wavelength excursion.

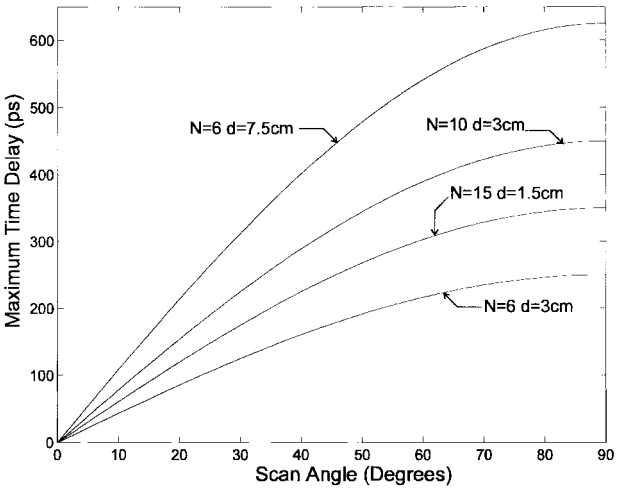

Fig. 3. Maximum time delay as a function of broadside scanning angle for different combinations of number of elements (N) and antenna spacing (d).

The wavelength output of each laser (λ_i) may be tuned around its center position, allowing a relative time-delay range of $[-\tau_{\mathrm{MAX}}, \tau_{\mathrm{MAX}}]$, as is schematically shown in Fig. 2. In fact, only $N-1$ lasers need to be tunable. For a N-element linear PAA, the maximum delay to be implemented is

$$\tau_{\mathrm{MAX}}(\mathrm{ps}) = 16.7 * (N-1) * d(\mathrm{cm}) * \sin(\Theta_{\mathrm{MAX\text{-}SCAN}}) \tag{1}$$

where d is the antenna-element separation and $\theta_{\mathrm{MAX\text{-}SCAN}}$ is the maximum scan angle relative to broadside direction. For broad-bandwidth PAA, the typical element spacing is $\lambda_{\mathrm{MIN}}/2$, where λ_{MIN} is the microwave wavelength corresponding to the highest frequency. As an example of (1), for an $N = 10$ element spaced as $d = 3$ cm using a maximum RF frequency (f_{RFMAX}) of 5 GHz, and scanning between $\pm$ 45°, the maximum delay (τ_{MAX}) required is 320 ps. Fig. 3 shows the maximum time delay as a function of the maximum scan angle taking f_{RFMAX} and N as parameters. From Fig. 3, it can be seen that for a maximum delay of $\pm$ 250 ps at each element, a six-element linear PAA with a f_{RFMAX} of 2 GHz may be scanned $\pm$ 25°, and this figure changes to $\pm$ 35° for $N = 10$ and a f_{RFMAX} of 5 GHz and $\pm$ 45° for 15 elements and a f_{RFMAX} of 10 GHz.

When all the lasers are tuned to their center wavelengths, the main lobe of the pattern array has to be pointed to broadside direction. The broadside direction would require a zero time delay between all the N antenna elements. Therefore, an extra standard single-mode fiber length (L_i) needs to be added to each antenna-element branch in order to compensate for the time delay at the corresponding center-position wavelength (λ_i), as shown in Fig. 1. The value of L_i as a function of the mean FBG group-delay slope δ, the wavelength separation between center positions $(\lambda_i - \lambda_1)$, and fiber refractive index (n_0) may be expressed as

$$L_i(\mathrm{cm}) = \delta(\mathrm{ps/nm}) * (\lambda_i(\mathrm{nm}) - \lambda_1(\mathrm{nm})) * \frac{0.03}{n_0}. \tag{2}$$

When the extra fiber lengths are added, the system-delay response is no longer a constant positive slope function, but a sawtooth response.

The wavelength excursion needed at any laser depends on the maximum expected time delay and the FBG group-delay response (ps/nm); for linear chirped this excursion is

$$\Delta\lambda(\mathrm{nm}) = 33.3 * \frac{(N-1) * d(\mathrm{cm}) * \sin(\Theta_{\mathrm{MAX\text{-}SCAN}})}{\delta(\mathrm{ps/nm})}. \tag{3}$$

Assuming a separation between adjacent wavelengths of one-and-a-half times the used bandwidth, the maximum number of different-delay addressable antenna elements employing a chirped fiber grating with a total bandwidth $\Delta\lambda_{\mathrm{GRATING}}$ is

$$N_{\mathrm{MAX}} \approx \sqrt{\frac{\Delta\lambda_{\mathrm{GRATING}}(\mathrm{nm}) * \delta(\mathrm{ps/nm})}{50 * d(\mathrm{cm}) * \sin(\Theta_{\mathrm{MAX\text{-}SCAN}})}} \tag{4}$$

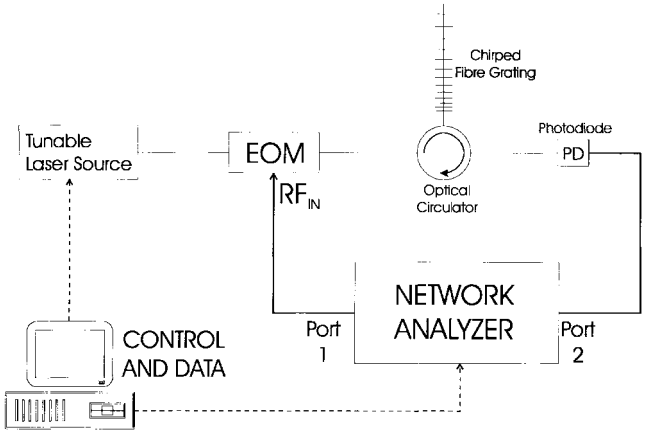

Fig. 4. Experiment setup for characterizing the relative time delays of one single branch of the TTD beamformer.

where expression of a constant group-delay slope has been assumed for the whole bandwidth $\Delta\lambda_{\mathrm{GRATING}}$.

III. Experiment

In order to demonstrate the principle described in Section II, a four-antenna-element PAA has been considered. The experimental setup is illustrated in Fig. 4, and corresponds to a single branch of the general scheme shown in Fig. 1. The FBG employed in this experiment is a 40-cm-long tapered linearly chirped grating with a linear group-delay response within a 4-nm bandwidth ($\Delta\lambda_{\mathrm{GRATING}} = 4$ nm) between 1547 and 1551 nm. The mean group-delay slope is 835 ps/nm. According to (4) and assuming a $\pm$ 45° scanning range, this grating would allow a maximum number of six elements for antenna elements equally spaced with a d of 3 cm. We will assume $N = 4$, $d = 4$ cm, and a full scanning range ($\pm$ 90°). From (1) and (3), a maximum delay (τ_{MAX}) of 200 ps and a wavelength excursion ($\Delta\lambda$) of nearly 0.5 nm are obtained. The center wavelengths for each laser/element are equally spaced and the following values were chosen $\lambda_1 = 1547.5$, $\lambda_2 = 1548.5$, $\lambda_3 = 1549.5$, and $\lambda_4 = 1550.5$ nm, respectively. These center wavelengths will need some compensating fiber length (L_i). Assuming a fiber refractive index (n_0) of 1.46, the theoretical values for these extra lengths are $\Delta L_1 = 0$ cm, $\Delta L_2 = 17.16$, $\Delta L_3 = 34.32$, and $\Delta L_4 = 51.47$ cm, respectively. The exact L_i values will be obtained from the actual group-delay FBG measurements.

In order to show the potential broad-bandwidth of the system, due to its TTD feature, the group-delay measurements were made at four different microwave frequencies (2, 5, 10, and 18 GHz) covering more than three octaves. The time delay for the full FBG bandwidth (1547–1551 nm) was measured at each microwave frequency.

Once the system time-delay response over the full bandwidth $\Delta\lambda_{\mathrm{GRATING}}$ is known, two parameters were extracted for each laser/element system branch. Namely, the mean delay at each center wavelength (relative time delay to λ_1) τ_i, which will be compensated by the corresponding extra fiber length L_i, and the relation between the time delay and the wavelength deviation around λ_i, which is assumed to be linear. This time-delay wavelength deviation is resumed in the slope δ_i at λ_i. Taking into account a 0.5-nm bandwidth around each λ_i and using a least-square linear approximation for all the four radio frequencies considered, the results shown in Table I were obtained. After compensating the time delay at the center wavelength λ_i, the time-delay measurements for each element (around the associated wavelength) for all four microwave frequencies are obtained as shown in Fig. 5. In Fig. 5, it may be observed that the time delay is as expected, i.e., almost linear and independent of the RF frequency. The pattern controller shown in Fig. 1 will use the slope parameter δ_i as reference for each laser tuning. Fig. 6 shows the time delay results that will be obtained at each antenna element for an input RF signal of 5 GHz as a function of the steering angle, considering that each tunable laser is driven according to the slope from Table I. The ideal expected results are also shown in Fig. 6, and it can be seen that the theoretical (ideal) results agree well with the experimental results. The rms error is given in Table II. The ripple around the ideal linear FBG group-delay response will introduce some error which should be considered for the system performance evaluation. The total-system time-delay error should be estimated assuming two main causes of error: the laser wavelength stability $\Delta\lambda_{\mathrm{LASER}}$ and the FBG time-delay response deviation from the linear slope $\sigma_{\mathrm{GRATING\text{-}SLOPE}}$. The laser wavelength stability can be translated to time precision by taking into account the grating response around each λ_i as

$$\sigma_{\mathrm{LASER}}(\lambda_i) = \Delta\lambda_{\mathrm{LASER}} * \delta_i. \tag{5}$$

The $\sigma_{\mathrm{GRATING\text{-}SLOPE}}$ parameter must be estimated over the full needed bandwidth, [0.5 nm. from (3)], around each center wavelength, and the standard deviation of the measurements from the linear approximation (slope δ_i at each λ_i) is calculated. Table II shows the results extracted from the measurements for all four wavelengths and for all four microwave frequencies. The mean standard deviation for each microwave frequency is also given. A total standard deviation of 3.31 ps would resume the time delay uncertainty due to the grating group-delay ripple. Taking into account both effects (laser wavelength stability and the FBG response) a total system precision can be estimated as

$$\sigma^2_{\mathrm{TOTAL}}(\lambda_i, f_{\mathrm{RF}}) = \sigma^2_{\mathrm{LASER}}(\lambda_i) + \sigma^2_{\mathrm{GRATING\text{-}SLOPE}}(\lambda_i, f_{\mathrm{RF}}). \tag{6}$$

The results for σ_{TOTAL}, assuming a laser wavelength stability of 0.01 nm, are shown in Table III. According to these results, the total system time-delay precision is 8.94 ps, which in turn implies a time-delay equivalent to a 16.1° phase error at 5 GHz or 6.44° at 2 GHz. These results are similar to the

TABLE I
RMS Time Delay and Slope at Each Central Wavelength for Four Different Microwave Frequencies ($\Delta\lambda = 0.5$ nm)

λ_i (nm.)	Mean Relative Time Delay (ps.) at λ_i	Compensating Length, L_i (cm.)	Slope δ_i (ps./nm.)
1547.5	**0**	**0**	**787**
1548.5	**824.1**	**16.93**	**819**
1549.5	**1653.7**	**33.98**	**850**
1550.5	**2505.8**	**51.49**	**865**

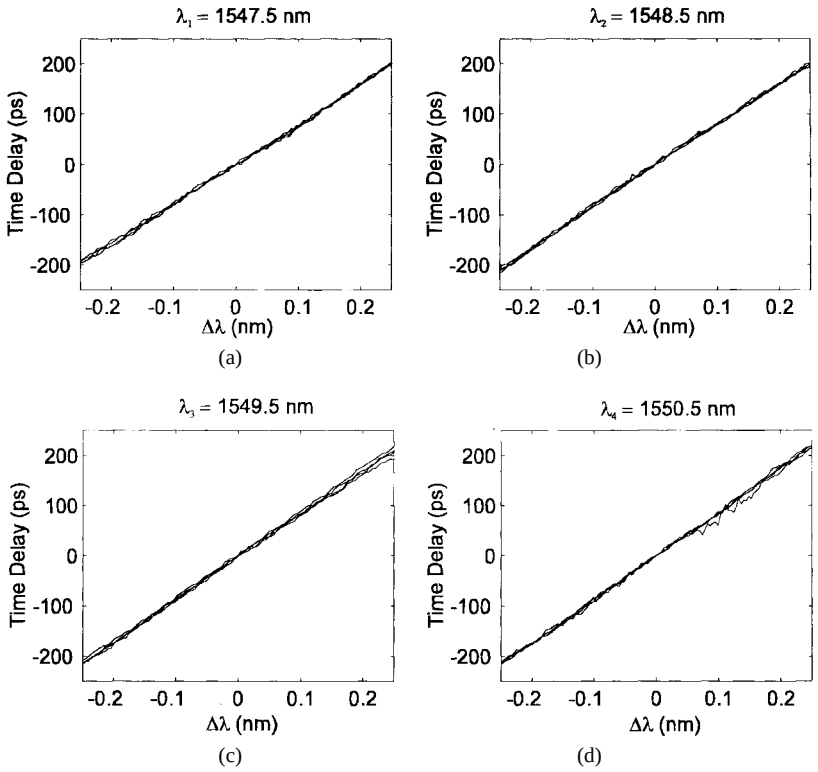

Fig. 5. Time-delay measurements at each antenna element for four different microwave frequencies (2, 5, 10, and 18 GHz) as a function of deviation from central wavelength ($\Delta\lambda$). Each figure corresponds to a different wavelength.

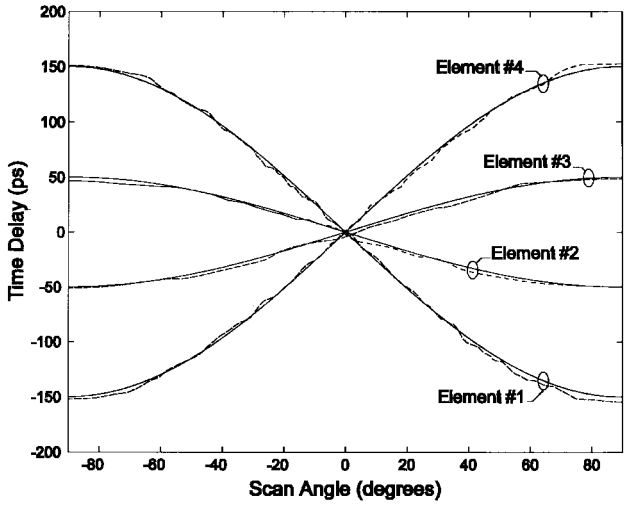

Fig. 6. Time-delay measurements (dashed lines) and theoretical results (solid lines) as a function of the scan angle when $f_{\mathrm{RF}} = 5$ GHz.

TABLE II
TIME-DELAY STANDARD DEVIATION FROM THE LINEAR RESPONSE (δ_i)

$\sigma_{\mathrm{GRATING\ SLOPE}}$	λ_1 1547.5 nm	λ_2 1548.5 nm	λ_3 1549.5 nm	λ_4 1550.5 nm	Mean σ
2 GHz	**3.87 ps.**	**3.83 ps.**	**2.90 ps.**	**4.04 ps.**	**3.69 ps.**
5 GHz	**2.81 ps.**	**3.37 ps.**	**2.49 ps.**	**2.53 ps.**	**2.82 ps.**
10 GHz	**3.02 ps.**	**2.99 ps.**	**2.01 ps.**	**2.27 ps.**	**2.61 ps.**
18 GHz	**2.59 ps.**	**2.35 ps.**	**3.39 ps.**	**6.17 ps.**	**3.93 ps.**

TABLE III
TOTAL RMS TIME-DELAY ERROR, TAKING INTO ACCOUNT THE GRATING GROUP-DELAY RESPONSE AND THE LASER WAVELENGTH STABILITY

σ_{TOTAL}	λ_1 1547.5 nm	λ_2 1548.5 nm	λ_3 1549.5 nm	λ_4 1550.5 nm	Mean σ
2 GHz	**8.77 ps.**	**9.05 ps.**	**8.98 ps.**	**9.55 ps.**	**9.09 ps.**
5 GHz	**8.35 ps.**	**8.86 ps.**	**8.86 ps.**	**9.01 ps.**	**8.77 ps.**
10 GHz	**8.42 ps.**	**8.72 ps.**	**8.73 ps.**	**8.94 ps.**	**8.71 ps.**
18 GHz	**8.28 ps.**	**8.51 ps.**	**9.15 ps.**	**10.6 ps.**	**9.19 ps.**

precision of a 3.5-b microwave digital phase shifter operating at 5 GHz, or a 5-b microwave digital phase shifter operating at 2 GHz.

In this experiment, the time-delay error comes due mainly to the laser wavelength stability. Therefore, just a little improvement in the laser wavelength stability will yield impressive results. For instance, a laser stability reduction to half its value ($\Delta\lambda_{\mathrm{LASER}} = 0.005$ nm) provides a total time-delay rms-error value of 5.31 ps, which is equivalent to a 3.8° phase rms error operating at 2 GHz (almost a 6-b microwave phase-shifter resolution).

In a second experiment, we insert 23 km of standard single-mode fiber between the optical circulator and the EOM, which results in converting the system dispersion of the 835-ps/nm grating in an equivalent grating with a dispersion of 430 ps/nm. The main effect of the equivalent dispersion change on the scheme is to provide a broader bandwidth $\Delta\lambda_i$ for the same maximum time-delay τ_{MAX}, and thus the sensitivity of the laser wavelength stability is reduced. Assuming an array antenna with $N = 4$, $d = 4$ cm, and a $\pm$ 45° scanning angle, a maximum delay (τ_{MAX}) of 140 ps and a wavelength excursion ($\Delta\lambda$) nearly 0.65 nm are obtained from (1) and (3). The measurements were made only for a microwave frequency

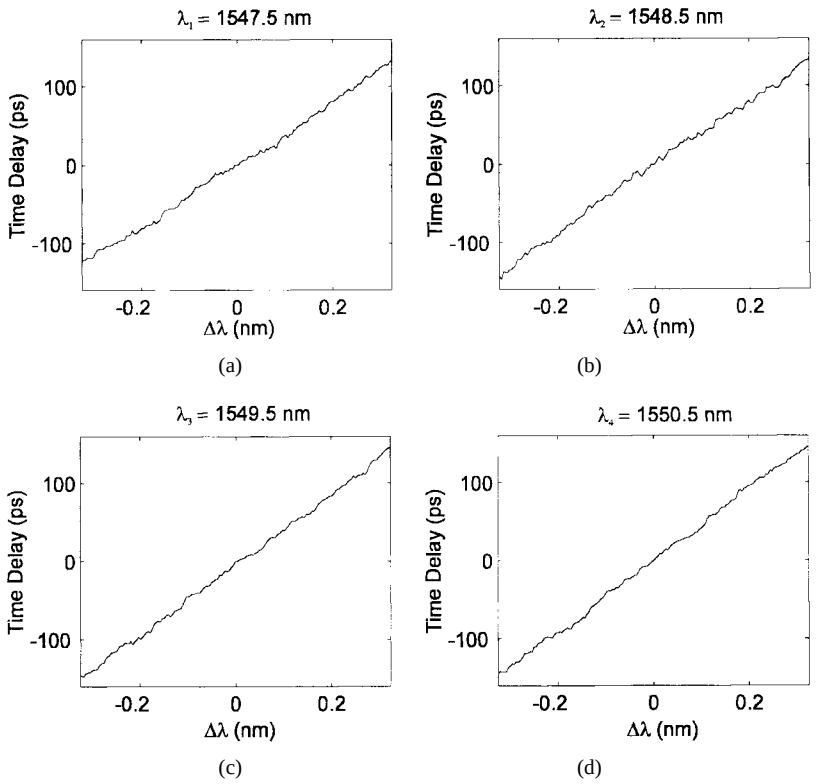

Fig. 7. Time-delay measurements at each antenna element at 2 GHz as a function of deviation from central wavelength ($\Delta\lambda$) for a different grating slope (430 ps/nm).

TABLE IV
RESULTS SUMMARY FOR THE 430 PS/NM EQUIVALENT FBG

λ_i (nm.)	Compensating Length, L_i (cm.)	Slope δ_i (ps./nm.)	$\sigma_{GRATING\ SLOPE}$	σ_{TOTAL}
1547.5	**0**	**396**	**3.27 ps.**	**5.13 ps.**
1548.5	**8.63**	**416**	**3.58 ps.**	**5.49 ps.**
1549.5	**17.31**	**449**	**2.45 ps.**	**5.12 ps.**
1550.5	**26.59**	**463**	**3.11 ps.**	**5.58 ps.**

of 2 GHz. The results (L_i, δ_i, σ_{TOTAL}, $\sigma_{\mathrm{GRATING\text{-}SLOPE}}$) are summarized in Table IV. The corresponding time-delay measured responses at each center wavelength λ_i are shown in Fig. 7. As expected, the total rms-time error for a laser wavelength stability of 0.01 nm is reduced to 5.3 ps, which is equivalent to a 3.8° rms phase error at 2 GHz, as a result of the reduced slope of the time delay response. On the other hand, a broader bandwidth is required than that in the previous experiment, which will impact on reducing the maximum number of elements of the PAA for a fixed full-grating bandwidth.

IV. REMARKS AND DISCUSSION

The results obtained and presented in Section III confirm the expected good performance employing the proposed optical beamforming scheme. That results may even be improved with specifically tailored FBG, which should be more focused on achieving very low group-delay response ripple instead of a highly linear response as required for dispersion compensation applications. The effects of mechanical features such as bending and coiling the grating on the performance have not been evaluated in this experiment, even though this does not represent any additional constraint in real PAA systems in which the optical feeder may be kept fixed.

Opposed to previously proposed optical beamformers which employ only one broad-bandwidth tunable laser [3], or several fixed multiwavelength sources [2], the phase pattern at the antenna element's plane is not limited to the linear phase one. For a particular PAA application in which a linear phase distribution is specified, the system requirements are reduced, as the maximum time delay for each element is no longer the same, but depends on the element position to the antenna geometrical center. Therefore, the associated optical bandwidth ($\Delta\lambda_i$) is different for each element and it is not necessary to be designed for the worst case, as in the simple experiment shown here.

The effect of the N tunable lasers on the overall system cost is not dramatic because the lasers do not require a broad tuning bandwidth, but just tenths of a nanometer, which should reduce its cost. The use of just one FBG for the whole system is a clear advantage compared to previous TTD schemes proposed, since mismatches in the numerous gratings may result in important inaccuracies.

The laser wavelength stability has been proved to have a very high effect on the whole system performance, and its reduction will be a very important issue for the development of future beamformers.

The maximum number of antenna elements for the proposed beamformer is currently limited to a few tenths of a nanometer for frequencies between L-band an X-band, but the available FBG lengths are growing from one day to the other, so the 40-cm-long fiber grating employed in the experiment will be

considered short in a few months. Furthermore, the group-delay grating response employed in our approach is by no means limited to a linear behavior as it is for dispersion compensating applications. The more stringent requirement is the delay response ripple. Some other group-delay responses are currently under study.

The dispersion-generated time delay is accompanied by dispersion-induced signal distortion as it is in the previously proposed systems using very long dispersive fiber lengths [2]–[4]. The substitution of the unchirped FBG's at the demultiplexing stage with inverse-slope chirped FBG's would mostly reduce this undesired effect. Furthermore, the high selectivity (typical values of the rejection ratios are 35 dB between channels with a band-guard 0.5 times the bandwidth) provided by the FBG filters used at the WDM would drastically reduce the effect of potential crosstalk interference.

V. Conclusion

To the best of our knowledge, the first demonstrated continuous TTD beamforming with wide-bandwidth chirped FBG, suitable for arbitrary antenna-element phase distribution is presented in this paper. A 40-cm-long chirped FBG has been used as the only dispersive element of the system, and it has been proved to potentially drive a four-element wide-bandwidth PAA with high resolution (6 bit) at L-band and S-band. Inaccuracies due to the wavelength stability of lasers and the linearity of the chirped grating group delay have also been considered, and their impact on the PAA performance is reported.

References

[1] A. Seeds, "Optical technologies for phased array antennas," *IEICE Trans. Electron*, vol. E76-C, no. 2, pp. 198–206, 1993.

[2] D. T. K. Tong and M. C. Wu, "A novel multiwavelength optically controlled phased array antenna with a programmable dispersion matrix," *IEEE Photon. Technol. Lett.*, vol. 8, pp. 812–814, June 1996.

[3] R. D. Esman *et al.*, "Fiber-optic prism true time-delay antenna feed," *IEEE Photon. Technol. Lett.*, vol. 5, pp. 1347–1349, Nov. 1993.

[4] M. Y. Frankel, P. J. Matthews, and R. D. Esman, "Two-dimensional fiber-optic control of a true time-steered array transmitter," in *IEEE MTT-Symp. Dig.*, San Franciso, CA, 1996, pp. 1577–1580.

[5] D. T. K. Tong and M. C. Wu, "Programmable dispersion matrix using Bragg fiber grating for optically controlled phased array antennas," *Electron. Lett.*, vol. 32, pp. 1532–1533, 1996.

[6] A. Molony *et al.*, "Fiber grating time delay element for phased array antennas," *Electron. Lett.*, vol. 31, pp. 1485–1486, 1995.

[7] R. A. Soref, "Fiber grating prism for true time delay beamsteering," *Fiber Integr. Opt.*, vol. 15, pp. 325–333, 1996.

[8] M. J. Cole, H. Geiger, R. I. Laming, S. Y. Set, M. N. Zervas, W. H. Loh, and V. Gusmeroli, "Continuously chirped, broadband dispersion-compensating fiber gratings in a 10 Gbits/s 110 km standard fiber link," presented at the *22nd ECOC Comm.*, Oslo, Norway, 1996.

J. L. Corral was born in Zaragoza, Spain, on April 20, 1969. He received the Ingeniero de Telecommunicacion degree with First Class Honours from the Universitat Politecnica de Valencia, Valencia, Spain, in 1993, and is currently working toward the Ph.D. degree there.

During 1993, he was Assistant Lecturer at the Departamento de Comunicaciones, Universitat Politecnica de Valencia. From 1993 to 1995, he was at the Microwave Technology and Equipment Section (XRM), at the European Space Research and Technology Centre (ESTEC) from the European Space Agency (ESA), where he was engaged in research on MMIC-based technologies and photonics technologies for on-board phased-array antennas. In 1995, he became an Assistant Lecturer in the Departamento de Comunicaciones, Universitate Politecnica de Valencia. His research interests include phased-array antennas, optical beamforming networks, microwave and millimeter-wave optical fiber systems.

J. Martí (S'89–M'92) received the Ingeniero Tecnico de Telecomunicacion and the Ingeniero de Telecommunicacion degrees from the Universidad Politecnica de Catalunya, Spain, in 1988 and 1991, respectively, and the Doctor Ingeniero de Telecomunicacion degree from the Universidad Politecnica de Valencia, Valencia, Spain, in 1994.

From 1989 to 1990, he was an Assistant Lecturer at the Escuela Universitaria de Valencia, Barcelona, Spain. He joined the Departamento de Comunicaciones at the Universidad Politecnica de Valencia in 1991, where he worked with the Optical Communications and Photonic Engineering Group. From 1991 to 1994, he was a Lecturer with the telecommunication engineering faculty, and became an Associate Professor in 1995. During 1994, he was a Visiting Research Fellow at the Electronics Laboratories, University of Kent, U.K., where he worked for three months with the Optical Communications Group. He has published over 50 papers in international technical journals in the fields of OFDM and SCM lightwave systems, optical processing of microwave signals, dispersion and fiber nonlinearities compensation employing fiber gratings and other techniques, and mobile and satellite communication systems. His current technical interest includes microwave/millimeter-wave fiber radio systems, dispersion compensation in analog and digital optical transmissions employing apodized linearly chirped gratings and optical phase conjugation, and multiple-access broad-band optical communication networks.

Dr. Martí is a member of several societies of IEEE, and is also a member of the Advisory Board of Journal of Fiber and Integrated Optics, in which he acted as guest editor of a special issue on multiplexing and demultiplexing in multiple-access optical networks. He has acted as reviewer of several IEEE journals and leading conferences. He was the recipient of the Doctorate Prize of the Telecommunication Engineer Association of Spain for his Ph.D. dissertation on optical prefiltering in SCM systems.

S. Regidor, photograph and biography not available at the time of publication.

J. M. Fuster, photograph and biography not available at the time of publication.

R. Laming received the degree in mechanical engineering with first class honors from Nottingham University, U.K., in 1983, and the Ph.D. degree from Southampton University, Southampton, U.K., in 1990.

In 1994, he joined the Optoelectronics Research Centre, Southampton University, where he is a Reader. Since this time, he has been conducting research into fiber devices and optical communications, which has resulted in many patents and approximately 200 publications. He has contributed many invited papers at international conferences. His current research interests include fiber amplifiers, gratings and devices, dispersion compensation, soliton generation, and fiber sensors.

Dr. Laming is a Chartered Engineer (CEng MIEE). He has served on the organizing committee of several international conferences and is a member of the IEE Professional Group E13, as well as associate editor for two journals. He is the recipient of the 1989 Marconi International Fellowship, Young Scientist of the Year Award, as well as a 1997 Royal Academy of Engineering Silver Medal, and with co-workers, recipient of the 1991 IEE Measurements Prize, and a 1996 Metrology for World Class Manufacturing Award.

M. J. Cole was born in Southampton, U.K., on August 20, 1971. He received a degree in electronics with first-class honors from the University of Sussex, U.K., in 1995. He is currently working toward the Ph.D. degree at the University of Southampton, Southampton, U.K.